Surfactant Assisted Synthesis of Homogeneous Calcium Based CO₂ Sorbent at Room Temperature

Chee Yew Henry Foo, Abdul Rahman Mohamed[*], Keat Teong Lee and Dahlan Irvan

Low Carbon Economy (LCE) Research Group, School of Chemical Engineering, Universiti Sains Malaysia, Engineering Campus, Seri Ampangan, 14300 Nibong Tebal, Pulau Pinang, Malaysia

Abstract: Calcium oxide (CaO) sorbents have been recently used for removal of CO₂ gases in fossil fuel-fired power plant. However, there are some limitations of CaO in CO₂ capturing such as rapid loss of activity during the capture cycles, which is a result of sintering, attrition, and consequent elutriation. Therefore, this paper has demonstrated a novel synthesis method to produce CaO at room temperature to avoid abovementioned drawbacks. In addition, introduction of ionic surfactant of sodium dodecyl sulfate to the CaO formation solution has shown a positive result of formation of homogeneous spherical particle with a mean Z-average diameter of 345.2 nm and polydispersion index (PDI) of 0.335 by dynamical light scattering measurement. Subjected to a high calcination temperature of 1200°C, developed CaO is able to maintain a CO₂ uptake capacity of 0.1025 g_{CO2}/g_{sorbent} under 30 minutes of carbonation time. Despite its lower CO₂ uptake capacity compared to maximum theoretical limit of 0.78 g_{CO2/gsorbent}, CaO particles is able to withstand a high calcination temperature of 1200°C and reported a particle size distribution ranged from 0.4 - 1.2μm after calcination which is just slightly larger than fresh developed CaO. Given that such small narrow distributed size of CaO, developed CaO at room temperature is good for packed-bed reactor in calcium looping processes and more studies are required to find a suitable support for fluidized bed reactor type. This successful synthesis story of CaO particle at room temperature has unraveled the possibility to develop nanosized CaO at room temperature in order to achieve high CO₂ uptake capacity while enjoying its superior thermal stability over multiple carbonation/calcination cycles.

Keywords: Calcium oxide, carbon capture, high temperature reaction, next generation CO₂ sorbent, thermal stability.

INTRODUCTION

Fossil-fuel-burning power plant accounts for approximately one third of anthropogenic CO₂ emissions which leads to global warming [1]. Carbon capture and storage (CCS) has received considerable attention as an option to reduce CO₂ emissions from such power plants [2]. However, none of these activities will be possible unless CO₂ is first captured. Ironically, none of the currently available CO₂ capture processes are economically feasible on a national implementation scale to capture CO₂ for sequestration, since they consume large amounts of parasitic power and significantly increase the cost of electricity. The most technologically-mature CO₂ capture method is through chemical absorption using amine-based sorbents, such as monoethanolamine (MEA) [3]. However, there are some prominent problems have to be solved before reaching full commercialization. Studies pointed out that degradation of amine-based sorbents at higher temperatures, reactions with undesired compounds (i.e. oxygen and sulphur dioxide), and corrosive nature have hindered this sorbent for being cost effective [4]. Therefore, these shortages discussed above that have led to scientists

investigating other alternatives of CO₂ capture, such as the reversible gas-solid reaction between calcium oxide and carbon dioxide to form calcium carbonate (the calcium looping cycle). This cycle was first explored in 1995 by Shimizu *et al*. [5] using lime-based chemistry for CO₂ capture but lately has a wider application in hydrogen production *via* the enhanced water gas shift reaction. This innovative technology seeks to demonstrate a technology to efficiently produce a pure hydrogen stream from coal gasification products with an integrated capture of carbon dioxide. Its principle is simple, that a calcium oxide sorbent is used, typically from limestone, reacting *via* the exothermic process which readily goes to completion under a wide range of conditions and repeatedly cycled between carbonation and calcinations vessels as shown in Figure **1**. In the first vessel, gasification of coal occurs, forming methane gas as a feedstock to undergo water gas shift. The methane gas formed is then channeled to carbonation vessel where water shift reaction and carbonation take place. All primary reactions of interest were written as below.

$$C_{2(s)} + 2H_{2(g)} \rightarrow CH_{4(g)}$$
$$\Delta H_{r,298K} = -74.9\ kJ/mol$$

Eq. (1)

$$CH_{4(g)} + H_2O_{(g)} \rightarrow CO_{(g)} + 3H_{2(g)}$$
$$\Delta H_{r,298K} = +206.193\ kJ/mol$$

Eq. (2)
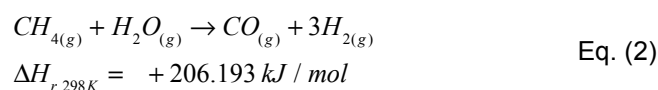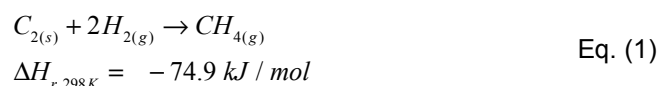
*Address correspondence to this author at the Low Carbon Economy (LCE) Research Group, School of Chemical Engineering, Universiti Sains Malaysia, Engineering Campus, Seri Ampangan, 14300 Nibong Tebal, Pulau Pinang, Malaysia; Tel: +604-5996410; Fax: +6045941013; E-mail: chrahman@usm.my

$$CO_{(g)} + H_2O_{(g)} \rightarrow CO_{2(g)} + H_{2(g)}$$

$$\Delta H_{r,298K} = -41.166 \, kJ/mol \qquad \text{Eq. (3)}$$

$$CaO_{(s)} + CO_{2(g)} \rightarrow CaCO_{3(s)}$$

$$\Delta H_{r,298K} = -178 \, kJ/mol \qquad \text{Eq. (4)}$$
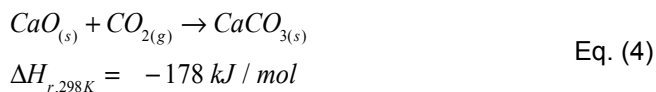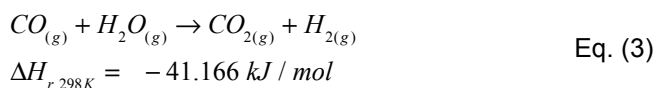
Unfortunately, based on the current state-of-art technology [6], spent sorbent has to be replaced by fresh sorbent incessantly due to sintering during regeneration process. Apart from that, the conditions in both carbonator and calciner must be a compromise between the increased rate of reaction obtained at higher temperatures and the reduced rate of degradation of sorbent at lower temperatures. Furthermore, degradation of sorbent due to contact with other impurities such as ash and sulphur will lower the efficiency in the fuel burned. Therefore, this paper aims to study the possibility to synthesis homogeneous calcium oxide particles at room temperature to reduce the effect of sintering (compared to conventional high temperature calcination step of $CaCO_3$ at >800°C to produce CaO) and high selectivity towards CO_2 gases. Moreover, a comprehensive characterization on this material was performed.

MATERIALS AND METHOD

Chemicals: sodium oxide (97%), calcium chloride (97%), anhydrous methanol (100%), Chloroform (97%) and sodium dodecyl sulfate (97%) were purchased from Aldrich. All chemicals were used without further purification.

Syntheses: In a typical synthesis, calcium chloride (0.015 mol) was dissolved in anhydrous methanol to produce solutions 1 (400 ml). To obtain monodispersed nanoparticles, SDS ionic surfactant (0.01 mol) was added to solution 1 before the addition of solution 2. To accelerate the dissolution process, solution 1 was sonicated in a bath to promote full dissolution of added salts. Following this, an stoichiometrically equal amount of Na_2O (0.015 mol) was dissolved by sonication in another portion of anhydrous methanol (100ml) to give solution 2. Solution 1 and 2 were mixed under rigorous stirring for 12 h. All reactions were conducted in sealed vessels at room temperature. The resulting precipitates were aged in the mother liquor at room temperature for 12 h until complete conversion/precipitation. The final products were washed and centrifuged several times with methanol and subsequently chloroform for rapid drying. The wet products were dried at 60°C overnight in oven.

Material Characterization

Powder X-ray diffraction (Bruker, AXS D8 Advance) was used to perform both quantitative and qualitative analyses on CaO's crystals. By using JADE software packages from MDI, quantitative analysis on multi-phase patterns was determined by means of reference intensity ratio (RIR value) method. In addition, qualitative analysis was also conducted to identify available phases, percentage of crystallinity, crystallite size (Scherrer equation) and strain. All collected diffraction patterns were measured by X-ray diffractometer that equipped with a Lynxeye
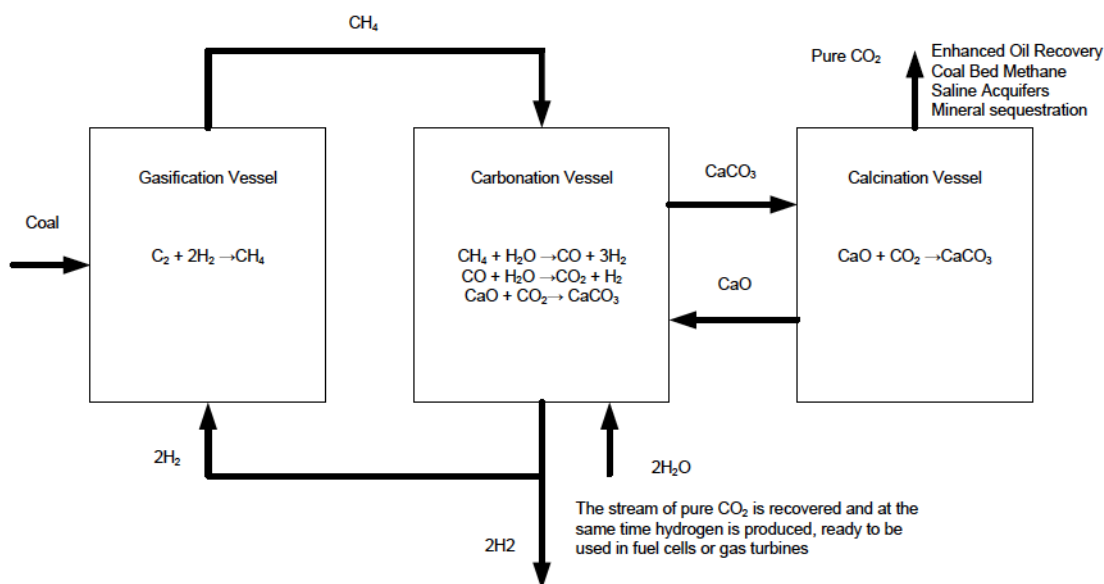
Figure 1: An overall process flow diagram of in situ CO_2 removal of water gas shift reaction to produce hydrogen as fuel.

superspeed detector and operated at 40 mA and 40 kV using Cu Ka radiation. The diffraction patterns were recorded at ambient conditions in the range of 2θ = 10-90°. The step size was 0.03° with a time duration per step of 0.8s.

FESEM/Zetasizer

Particle size and surface morphology was characterized using scanning electron microscopy (FEI Quanta 450 FEG, Eindhoven, NL). A double-sided carbon tape was used to attach the material onto brass stub. All images were taken at a magnification of 10000x. Observation is conducted at 10kV electron beam's power with a secondary electron image detector. Particle size distribution (limited to particles size less than $1 \mu m$) and polydisperity of different precursors were determined by a dynamic light scattering method using Zetasizer software by Zetasizer Nano-ZS90 (Malvern Instruments, UK) at 25°C. Prior to dyanmic light scattering test, sample powder was first dispersed in pure ehtylene glycol solution, ultrasonicated (10 minutes) and syringe filtered (400µm) before measurement.

EDX

To determine the chemical composition of samples, an energy dispersive X-ray (EDX) analysis was conducted. It is a technique by which the elemental composition of the sample can be identified. The EDX analysis system works as an integrated feature of a scanning electron microscope (FEI Quanta 450 FEG, Eindhoven, NL). Briefly, samples spread on the metal stub and platinum coating was carried out. The samples were then examined under a scanning electron miscroscope. From the samples or from different areas of the sample, the elemental composition were determined.

CO$_2$ Absorption Analysis

The CO$_2$ uptake characteristics of CaO derived from surfactant assisted homogeneous CaO particles synthesis was evaluated in a simultaneous TGA/DSC analyzer (TA instrument, SDT Q600). In a typical carbonation study, the following protocol was used. A small amount (<20mg) of sample was placed in an alumina pan (90uL). Prior to any carbonation study, pre-adsorbed CO$_2$ and H$_2$O from atmosphere was removed by heating the sample from room temperature to 1200°C in a flow of purified N$_2$ (99.99% purity, 100mL/min flow rate, 10°C/min heating rate). The

sample was then cooled to a studied carbonation temperature (650°C). Once the carbonation temperature was reached and stabilized, purified CO$_2$ (99.99%) with a flow rate of 100 mL/min was introduced into the system while the differential change in the sample weight was recorded for 30 minutes.

The CO$_2$ uptake capacity was defined as Eq. 5 below but with an assumption that the mass increase due to N$_2$ physisorption on the sample was negligible and not taken into consideration.

$$CO_2 \text{ uptake capacity (mmolCO}_2\text{/g sorbent)} = \frac{(m_t - m_o)/44}{m_o} \times 1000 \qquad \text{Eq. (5)}$$

where 44 is the CO$_2$ molar weight (g/mol), and m_o and m_t are the sample weights at the beginning and time t of the carbonation reaction, respectively. Based on the theoretical limit of 17.85 mmol of CO$_2$ absorbed per gram of CaO, 30 minutes of carbonation time was chosen to represent a reasonable reactor size throughput.

RESULTS AND DISCUSSION

Particle Size Distribution and Thermodynamics Property

Figure **2** expressed dynamic light scattering (DLS) results in terms of the Z-average in volume percent with a maximum and minimum error bar. It should be noted that DLS provides statistical representative data about the hydrodynamic size of nanomaterials in Z-average value. This value should only be employed to provide the characteristics size of the particles if the suspension is monomodal (only one peak), spherical and monodisperse. Therefore, for a mixture of particles with obvious size difference (bimodal distribution), the calculated Z-average carries irrelevant size information. As shown in Figure **2**, CaO derived at room temperature fall in a size range of 140-750 nm with a mean value of 345.2 d.nm and respective PDI index of 0.335. This PDI index is fall in the range of 0.08 – 0.7 which is suitable for DLS measurement. Hence, it is reasonable to assume a homogeneous spherical shape and size of CaO particles for the following calculation.

Critical Packing Parameter and Gibbs Free Energy

Israelachvii (1976) [7] proposed a critical packing parameter (cpp) to describe the surfactant molecule structures as:
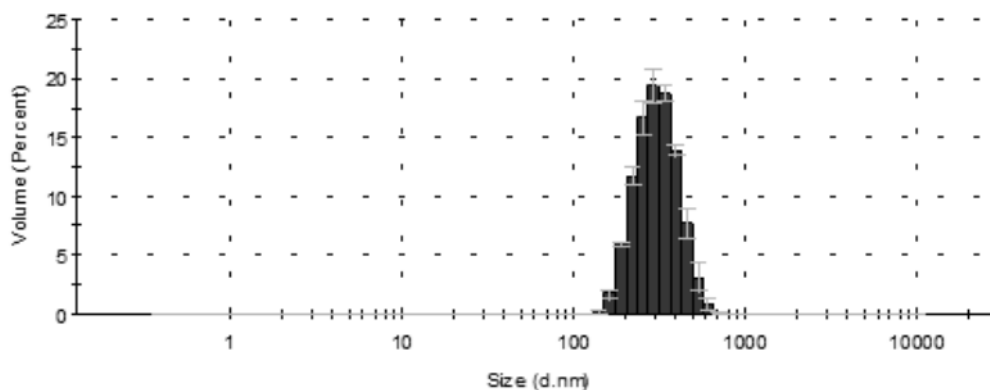
Figure 2: Particle size distribution of SDS assisted CaO particles synthesized at room temperature.

$$cpp = \frac{v}{a_o l_c} \qquad \text{Eq. (6)}$$

where v denotes to the tail chain (or chains) volume, l_c is the critical tail chain length, a_o is the headgroup area at the head-tail interface. The v and l_c can be calculated by empirical equations (Tanford, 1980) while a_o can be measured by experimental method.

To obtain cpp value, first, micelles volume v of the hydrocarbon tail on the amphiphilic molecule was calculated based on Eq. (7).

$$v = [27.4 + 26.9\, n_c]\, A^3 \qquad \text{Eq. (7)}$$

where 27.4 A^3 equals the volume of the CH_3 methyl cap at the end of the chain. 26.9 A^3 the volume of each methylene (H-C-H) group along the chain, and n_c is the number of carbon atoms in the chain – 12 for SDS. With this hydrocarbon tail volume, we can calculate the micelles aggregation number N_o by the following Eq. (8).

$$N_o v = 4\pi\, R^3_{mic}/3 \qquad \text{Eq. (8)}$$

where the micelle hydrocarbon core of R_{mic} is measured by DLS analysis which is 172.6 nm.

On the other hand, the total area per amphiphilic molecule headgroup (a_o) at the surface of the hydrocarbon core is

$$a_o = 4\pi R^2_{mic}/N_o \qquad \text{Eq. (9)}$$

by taking R_{mic} = 172.6 nm and N_o = 61.5 x 10^6, a_o is determined at $0.62 A^2$. Subsequently, cpp value was calculated as 0.3279 which is fall in the category of spherical micelles indicating a SDS micelles at low salt solution.

Next, we can relate the critical micelles concentration (CMC) to the free energy of micelle formation by Eq. (10).

$$\Delta G_{mic} = RT \ln CMC \qquad \text{Eq. (10)}$$

where we can express the CMC in any concentration units, it is usually quoted as a mole fraction, that is $C_{surfactant}/(C_{surfactant} + C_{methanol})$ where $C_{methanol}$ = 24.7 mol/liter. Figure **3** shows the CMC value by studying the conductivity of methanol-SDS solution and CMC = 0.02 M was obtained. Therefore, ΔG_{mic} was found to be -17.6 kJ/mol which is very close to the value of ΔG_{mic} for SDS-water system of -20 kJ/mol.

Parameters of Surfactant Assisted CaO Growth

To study the growth rate of CaO at room temperature, weight of precipitated CaO particles in solution was measured after dried overnight in oven. To investigate the significant parameter that affect the growth of CaO particles, Design of Experiment (DOE) software was used to study the correlation between process parameters and growth rate of CaO particles. DOE was carried out based on the following process parameters: concentration of calcium precursor (0.03-0.3 M), Molar ratio of surfactant to calcium precursor (0.01-0.1), reaction time (5-30 minutes) and stirring speed (0-1000 rpm). Table **1** shows the growth rate of CaO particle from solution in various combination of process parameters generated by the program. The growth rate of CaO was found to range from 1.11 mg/min to 26 mg/min depending on the different combination of process parameters.

The results obtained from the experimental work using DOE were analyzed by multiple regression analysis to determine a suitable polynomial model that can best fit the results. Based on the F value and the
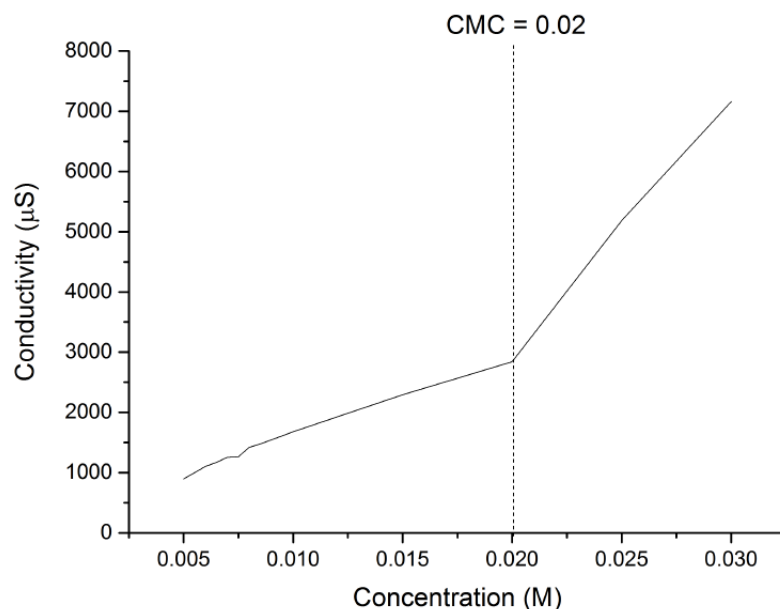
Figure 3: Critical micelles concentration by studying the conductivity of solution at various concentrations.

Table 1:   Generated DOE's Experimental Design Layout and Results of CaO Formation Rate

Std	Run	Block	Factor A: Concentration (M)	Factor B: Molar ratio	Factor C: Time (min)	Factor D: Stirring speed (rpm)	Response: Formation rate (mg/min)
25	1	Block 1	0.16	0.06	17.50	500	8.20
9	2	Block 1	0.10	0.03	11.25	750	5.15
1	3	Block 1	0.10	0.03	11.25	250	7.44
13	4	Block 1	0.10	0.03	23.75	750	3.38
30	5	Block 1	0.16	0.06	17.50	500	8.20
21	6	Block 1	0.16	0.06	5.00	500	26.00
20	7	Block 1	0.16	0.10	17.50	500	7.91
27	8	Block 1	0.16	0.06	17.50	500	8.20
18	9	Block 1	0.30	0.06	17.50	500	18.3
24	10	Block 1	0.16	0.06	17.50	1000	7.58
3	11	Block 1	0.10	0.08	11.25	250	7.28
15	12	Block 1	0.10	0.08	23.75	750	3.26
26	13	Block 1	0.16	0.06	17.50	500	8.20
14	14	Block 1	0.23	0.03	23.75	750	8.12
29	15	Block 1	0.16	0.06	17.50	500	8.20
10	16	Block 1	0.23	0.03	11.25	750	23.8
23	17	Block 1	0.16	0.06	17.50	0	7.37
12	18	Block 1	0.23	0.08	11.25	750	16.99
17	19	Block 1	0.03	0.06	17.50	500	1.11
7	20	Block 1	0.10	0.08	23.75	250	3.32
4	21	Block 1	0.23	0.08	11.25	250	17.55
5	22	Block 1	0.10	0.03	23.75	250	3.28
8	23	Block 1	0.23	0.08	23.75	250	7.53

(Table 1). Continued.

Std	Run	Block	Factor A: Concentration (M)	Factor B: Molar ratio	Factor C: Time (min)	Factor D: Stirring speed (rpm)	Response: Formation rate (mg/min)
2	24	Block 1	0.23	0.03	11.25	250	15.86
11	25	Block 1	0.10	0.08	11.25	750	6.44
28	26	Block 1	0.16	0.06	17.50	500	8.20
19	27	Block 1	0.16	0.01	17.50	500	6.49
22	28	Block 1	0.16	0.06	30.00	500	4.16
16	29	Block 1	0.23	0.08	23.75	750	8.14
6	30	Block 1	0.23	0.03	23.75	250	8.66

probability value, a quadratic model was suggested by the program for this purpose. The experimental data were analyzed using analysis of variance (ANOVA) at 95% confident interval (CI). Table **2** displays the ANOVA results for the process parameter of CaO growth at room temperature. The capability of the selected quadratic model to represent the real reaction process as well as the significance of all process parameters in affecting the growth rate of CaO were determined using F (Fisher)-test. If the calculated Prob > F value is less than 0.05, then the developed model representing the CaO growth rate and all the process parameters will be considered to have significant effect on the growth rate of CaO. As shown in Table **2**, F-test on the developed quadratic model gives a F value of and Prob > F value less than 0.0001, indicating that the developed model is significant at 95% CI. This indicates that the quadratic model selected was suitable to represent the actual reactive CaO growth rate. Among all the process parameters, only parameter A (calcium precursor concentration), C (reaction time), derivative terms of AC and C^2 were found to significantly affect the growth of CaO since their F values are higher than the theoretical value, $F_{1,15}$ of 4.54 at 95% CI. Such result reveals the fact that any changes in the value of these process parameters

Table 2:   ANOVA Results Based on a Quadratic Model Selection

Source	Sum of Squares	DF	Mean Square	F value	Prob > F
model	986.81	14	70.49	20.00	<0.0001[a]
A	429.09	1	429.09	121.78	<0.0001[a]
B	0.23	1	0.23	0.065	0.8026
C	404.26	1	404.26	114.73	<0.0001[a]
D	0.95	1	0.95	0.27	0.6108
AB	3.31	1	3.31	0.94	0.3476
AC	51.41	1	51.41	14.59	0.0017[a]
AD	6.94	1	6.94	1.97	0.1808
BC	0.49	1	0.49	0.14	0.7144
BD	2.30	1	2.30	0.65	0.4322
CD	1.07	1	1.07	0.30	0.5895
A^2	1.78	1	1.78	0.51	0.4877
B^2	3.78	1	3.78	1.07	0.3167
C^2	70.11	1	70.11	19.90	0.0005[a]
D^2	2.51	1	2.51	0.71	0.419
Residual	52.85	15	3.52		

$R2 = 0.9492$; Adjusted $R2 = 0.9017$; Predicted $R2 = 0.7072$.
[a]significant at 95% confident interval.
[b]not significant at 95% confident interval.

will bring significant changes to the growth of CaO consequently.

By eliminating the insignificant parameters, the multiple regression analysis gives the following quadratic model equation (in coded factor) that correlates the growth rate of CaO to the various process parameters as shown in Eq. (11):

$$\text{Growth rate} = 7.83 + 4.23A - 4.10C - 1.79AC + 1.65C^2$$
$$\text{Eq. (11)}$$

According to Eq. (11) obtained from the statistical analysis, the growth rate of CaO was positively affected by the following process parameters A and C^2; meaning an increase in the value of these parameters will enhance the growth rate of CaO. On the other hand, an increase in the value of C and AC will eventually reduce the growth rate of CaO since these parameters have negative effect on the growth rate of CaO in this particular process. Figure **4** shows the parity plot of the developed model. The predicted result from Eq. (11) is agree relatively well with actual experimental data with a R^2 of 0.8361 compared to R^2 value of 0.9492 deduced directly from ANOVA analysis.

Crystal Structure Analysis

In subject of crystallographic structure, the crystalline phases of all the fresh and calcined CaO were determined by XRD analysis and the XRD patterns of both samples are depicted in Figure **5**. Prior to XRD analysis, both fresh CaO and calcined CaO have been exposed to atmospheric moisture and CO_2 for three days before analysis. Fresh CaO displays broad peaks of the (001), (100), (011), (110), (111), (003), (201) and (202) for $Ca(OH)_2$ phase; (024) and (210) for Calcite phase; (110), (021), (012), (221) and (212) for aragonite phase; (111), (224), (321) and (402) for vaterie phase accordingly. While calcined CaO displays broad peaks of the (001), (100), (101), (102), (110), (201), (202), (210) and (104) for $Ca(OH)_2$ phase; (111), (200), (220), (311), (222), (400) and (331) for CaO phase respectively.

As labeled in Figure **5**, fresh CaO exhibited a severe degradation to $Ca(OH)_2$ and $CaCO_3$ after exposed to atmospheric moisture and CO_2 for 3 days. On the other hand, calcined fresh CaO shares similar pattern with conventional limestone derived CaO as majority consists of CaO planes. Surprisingly, calcined CaO only has phases of CaO and $Ca(OH)_2$ while fresh CaO has an additional phase of $CaCO_3$. Therefore, it is believed that CaO synthesized at room temperature has a higher selectivity towards CO_2 and capable of absorbing CO_2 at room temperature.

By performing a crystal refinement on both fresh and calcined CaO, parameters such as quantitative analysis, overall crystallinity, crystal size, and strain were calculated and tabulated in Table **3**. It is worth noting that the calculation of crystallinity by XRD is based on the presumption that the broad peak comes
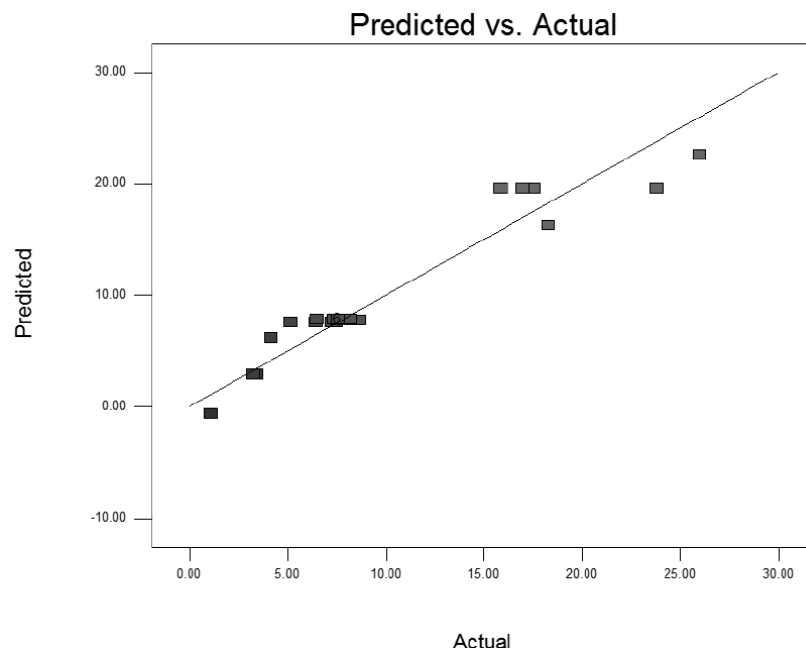
Figure 4: Parity plot of predicted versus actual value of a quadratic model and experimental results.
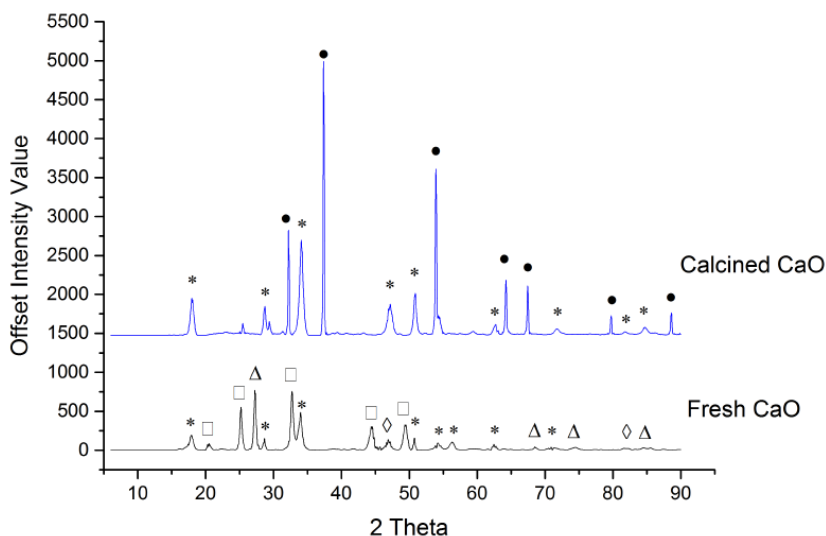
Figure 5: XRD patterns of fresh (3 days) and calcined CaO developed at room temperature.
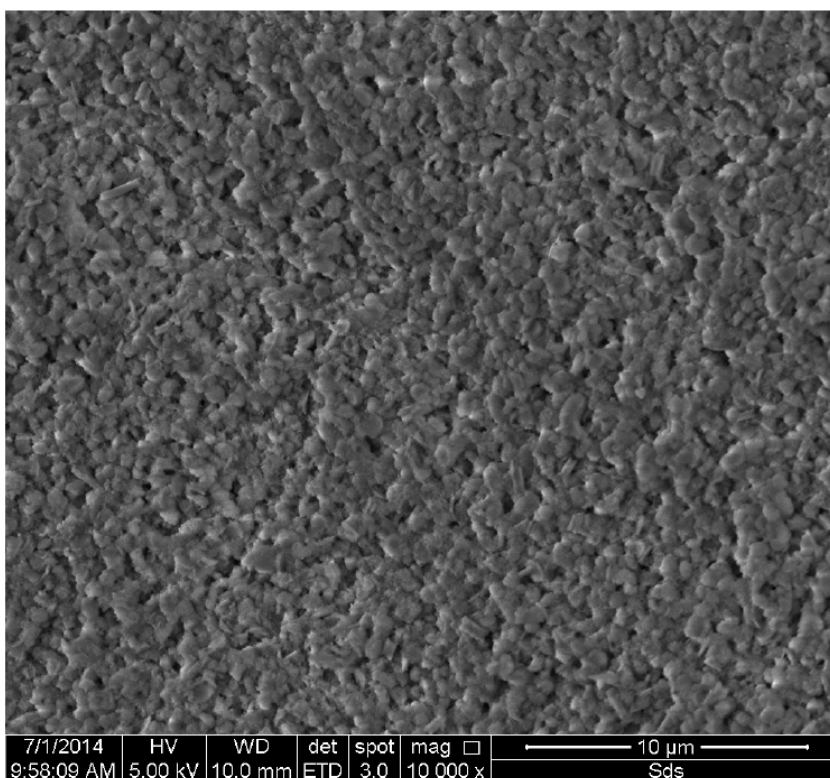
Figure 6: SEM image of calcined CaO at 1200°C.

from amorphous phase, the sharp peak comes from crystal phase. Defects such as dislocation, stacking faults, small crystalline size, will also cause broading of peaks and weak signal. Therefore, perfect crsytallinity material shows larger crystallite size, diffraction pattern shows sharper, stronger signal and symmetry peaks. Apart from that, XRD quantitative analysis is based on RIR value. The reference intensity ratio (RIR) method is a specific application of the internal standard method for quantitative XRD. The RIR is defined as the ratio of

the strongest peak of the unknown phase to that of an internal standard in an one-to-one mixture. Due to substantial lattice strain appeared in the specimen, which broaden the peaks as a function of 2θ angle differently than for small crystallites, the crystallite size and strain was simultaneously estimated using the FWHM values of fitted profiles. A least-square fit of the FW(S) values to determine the size and strain values using the following equation:

Table 3: **Interpretation of XRD Patterns to Obtain Quantitative Phase's Composition, Overall Crystallinity, Crystallite Size and Strain Values**

Quantitative analysis (weight percent)					
	CaO	**Ca(OH)₂**	**Vaterie**	**Calcite**	**Aragonite**
Fresh CaO	-	0.2	85.8	6.2	7.8
Calcined CaO	44.9	55.1	-	-	-
Crystallinity	Percentage	Residual error of fit (%)			
Fresh CaO	90.50	10.83			
Calcined CaO	90.43	11.05			
Size (nm)	CaO	Ca(OH)₂	Vaterie	Calcite	Aragonite
Fresh CaO	-	182	226	113	166
Calcined CaO	570	177	-	-	-
Strain	Percentage	ESD of fit			
Fresh CaO	0.608	0.00477			
Calcined CaO	0.189	0.00499			

$$FW(S) \times \cos(\theta) = K\lambda / size + 4 \times strain \times \sin(\theta) \qquad \text{Eq. (12)}$$

Notice that the formula turns into the famous Scherrer equation when the strain term is zero.

Surface Morphology

The structure of the calcined CaO was imaged using high-resolution scanning electron microscope (HR-SEM) as illustrated in Figure **6**. It shows that, calcined CaO is originally consists of mainly homogeneous sphere particles but slowly merging together into a network of larger particles as sintering dominated once calcined at high temperature (>600$^{\text{o}}$C). This network shows some cavities (channels) which are probably formed by the release of the CO_2 gas during calcination (prior to adsorption of atmospheric CO₂ by fresh precipitated CaO from methanol solution). It is believed that formation of channels and cracks contribute to an increase of the specific surface area which eventually increases the sorbent capacity to capture CO_2. Moreover, particle size distribution of calcined CaO was measured and tabulated in Figure **7**. It shows that calcined CaO particles are fall in a range of 0.4 – 1.2 μm which is slightly larger than fresh CaO (0.345 μm) measured by DLS technique.

EDX

An energy-dispersive X-ray (EDX) analyzer that attached to the scanning electron microscope was used for the elemental analysis of CaO sample. All elemental analysis results are tabulated in Table **4**.
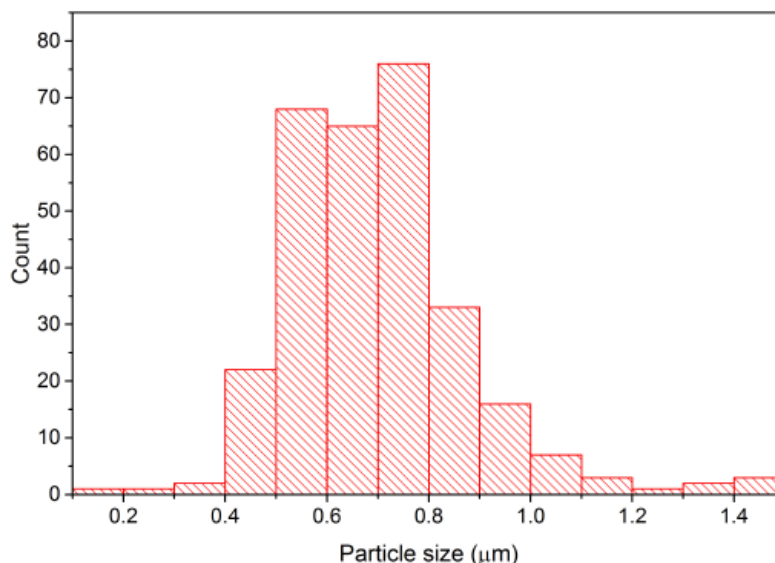
Figure 7: Particle size distribution of fresh CaO developed at room temperature.

Calcined CaO sample exhibit a majority amount of calcium based component consist of CaO, $CaCO_3$ and $Ca(OH)_2$ which is agreed well with XRD analysis. As depicted in Table **4**, composition of elements Ca, C, O, Cl and S are reported as 19.08%, 24.81%, 55.18%, 0.26% and 0.66% respectively. These small amounts of elements S and Cl indicated that additional washing steps with excess methanol and chloroform are required in order to completely remove unreacted components.

Table 4:   Result of EDX Elemental Analysis Measured at Atomic Percentage

Element	Atomic %
C	24.81
O	55.18
S	0.66
Cl	0.26
Ca	19.08

CO₂ Absorption Activity

The results on the CO_2 uptake capacity for room temperature derived CaO and commercial CaO are illustrated in Figures **8** and **9** respectively. It was observed that under 30 minutes of CO_2 sorption time, calcined CaO sample recorded a maximum CO_2 sorption capacity of 0.1025 gCO₂/gsorbent. Although it is much lower than theoretical limit of 0.78 gCO₂/gsorbent, calcined CaO sample has given us a new direction of improvement on conventional limestone derived CaO. First of all, it is possible to

synthesis CaO particles at room temperature without severe high temperature calcination step to convert $CaCO_3$ to CaO that lead to sintering effect. Secondly, SDS assisted synthesis method is capable of developing a homogeneous CaO particles even calcined at high temperature (1200°C). It is believed that such uniform particle size is essential for maintaining CO_2 uptake capacity without serious penalty when subjected to multiple carbonation and calcination cycles.

CONCLUSION

In this study we reported the successful story of synthesis of CaO based CO_2 sorbents using SDS assisted technique at room temperature. It was found that the initial concentration of calcium precursor and reaction time influenced the formation rate of the material most. Using SDS as stabilizing surfactant to the formation of CaO particles, a homogeneous size distribution of submicron ranged CaO has been developed. This developed CaO particles is highly reactive to atmospheric moisture and CO_2 as proven by XRD analysis where fresh CaO has been converted to $Ca(OH)_2$ and $CaCO_3$ after exposed to air for 3 days. Nevertheless, additional purification steps or sophisticated fully sealed reactor are required in order to avoid degradation of sample by atmospheric moisture and CO_2. Worth still, further investigation on fine tuning this synthesis process to develop nanosized CaO is recommended. This is because nanosized CaO is blessed with enormous active surface area for CO_2 absorption while keeping its thermal stability as nano-CaO synthesized at room temperature will avoid sintering problem happened at >600°C.
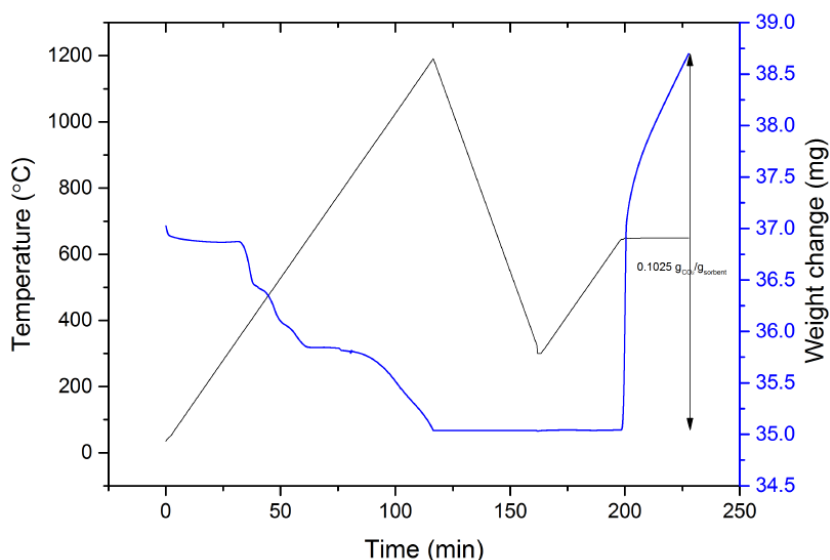
Figure 8: TGA curves of pre-heating at 1200°C and 30 minutes carbonation reaction at 650°C.
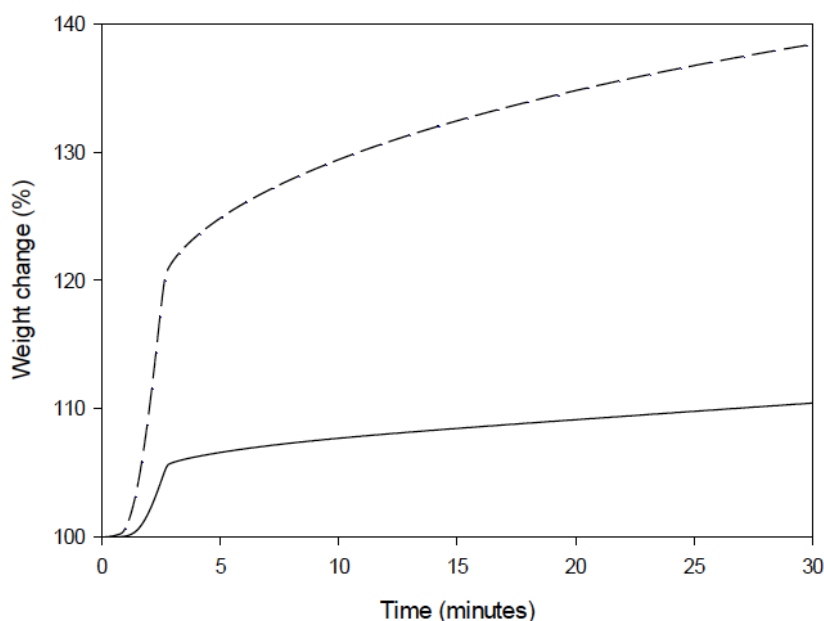
Figure 9: Recorded weight changes of commercial CaO (−) and developed CaO (--) during 30 mintues carbonation reaction at 650^oC.

REFERENCES

[1]   Solomon S, Qin D, Manning M, Chen Z, Marquis M, Averyt KB, Tignor M, Miller HL, Eds. Climate Change 2007: The Physical Science Basis. Contribution of Working Group I to the Fourth Assessment Report of the Intergovernmental Panel on Climate Change. Cambridge University Press. United Kingdom: Cambridge 2007.

[2]   Figueroa JD, Fout T, Plasynski S, McIlvried H, Srivastava RD. Advances in CO_2 capture technology – The U.S. Department of Energy's Carbon Sequestration Program. International Journal of Greenhouse Gas Control 2008; 2(1): 9-20.
        http://dx.doi.org/10.1016/S1750-5836(07)00094-1

[3]   Rao AB, Rubin ES. A technical, economic, and environmental assessment of amine-based CO2 capture technology for power plant greenhouse gas control. Environmental Science and Technology 2002; 36(20): 4467-4475.
        http://dx.doi.org/10.1021/es0158861

[4]   Lepaumier H, Picq D, Carrette P. New amines for CO2 capture. I. mechanisms of amine degradation in the presence of CO_2. Industrial and Engineering Chemistry Research 2009; 48(20): 9061-9067.
        http://dx.doi.org/10.1021/ie900472x

[5]   Shimizu T, Hirama T, Hosoda H, Kitano K, Inagaki M, Tejima K. A twin fluid-bed reactor for removal of CO2 from combustion processes. Chemical Engineering Research and Design 1999; 77(1): 62-68.
        http://dx.doi.org/10.1205/026387699525882

[6]   Manovic V, Anthony EJ. Lime-based sorbents for high-temperature CO2 capture-a review of sorbent modification methods. International Journal of Environmental Research and Public Health 2010; 7(8): 3129-3140.
        http://dx.doi.org/10.3390/ijerph7083129

[7]   Israelachvii JN, Mitchell DJ, Ninham BW. Theory of self-assembly of hydrocarbon amphiphiles into micelles and bilayers. Journal of the Chemical Society, Faraday Transactions 2: Molecular and Chemical Physics 1976; 72: 1525-1568.
        http://dx.doi.org/10.1039/f29767201525